Astron. Astrophys. 362, 69–74 (2000)

ASTRONOMY AND ASTROPHYSICS

On the peculiar X-ray properties of the bright nearby radio-quiet quasar PDS 456

C. Vignali[1,2], A. Comastri[2], F. Nicastro[3,4], G. Matt[5], F. Fiore[3,4,6], and G.G.C. Palumbo[1]

[1] Dipartimento di Astronomia, Università di Bologna, Via Ranzani 1, 40127 Bologna, Italy (vignali@kennet.bo.astro.it)
[2] Osservatorio Astronomico di Bologna, Via Ranzani 1, 40127 Bologna, Italy
[3] Harvard-Smithsonian Center of Astrophysics, 60 Garden Street, Cambridge MA 02138, USA
[4] Osservatorio Astronomico di Roma, Via Frascati 33, 00044 Monteporzio, Italy
[5] Dipartimento di Fisica, Università degli Studi "Roma Tre", Via della Vasca Navale 84, 00146 Roma, Italy
[6] BeppoSAX Science Data Center, Via Corcolle 19, 00131 Roma, Italy

Received 14 March 2000 / Accepted 21 August 2000

Abstract. BeppoSAX and ASCA observations of the nearby (z = 0.184), high–luminosity, radio-quiet quasar PDS 456 are presented. The X–ray spectrum is characterized by a prominent ionized edge at 8–9 keV (originally discovered by RXTE, Reeves et al. 2000) and by a soft excess below 1.5 keV. The lack of any significant iron Kα emission line suggests for the edge an origin from line–of–sight material rather than from reflection from a highly ionized accretion disc. The hard X–ray continuum is indeed well modelled by transmission through a highly-ionized medium with a large column density ($N_{\rm H_{warm}} \sim 4.5 \times 10^{24}$ cm^{-2}) plus an additional cold absorber with a lower column density ($N_{\rm H_{cold}} \sim 2.7 \times 10^{22}$ cm^{-2}).

Key words: galaxies: nuclei – galaxies: quasars: individual: PDS 456 – X-rays: galaxies

1. Introduction

The average 2–10 keV X–ray spectrum of low/medium-redshift quasars observed with EXOSAT (Comastri et al. 1992; Lawson et al. 1992), Ginga (Williams et al. 1992; Lawson & Turner 1997) and ASCA (Reeves et al. 1997; George et al. 2000) is well represented by a power law with a slope similar to that of lower luminosity Seyfert 1 galaxies ($\Gamma \simeq$ 1.9–2.0, Nandra & Pounds 1994) and significant dispersion around the mean value $\sigma \simeq$ 0.2–0.3. The typical imprints of reprocessing gas (i.e. the reflection "hump" and the Kα emission line), which characterize the spectra of Seyfert 1 galaxies (Nandra & Pounds 1994; Nandra et al. 1997) are however not present in high luminosity objects.

Indeed, only a small number of quasars have a spectrum more complex than a simple power law (plus, sometimes, a soft excess at low energies). This fact has been tentatively ascribed to different physical conditions of the accreting gas in the innermost regions surrounding high-luminosity quasars with respect to Seyfert galaxies. Iwasawa & Taniguchi (1993) suggested the existence (based on Ginga data) of an X–ray "Baldwin" effect, whereby the equivalent width of the iron Kα line decreases with luminosity. Nandra et al. (1997, 1999) have recently confirmed and extended this result using ASCA data. Both the profile and strenght of the Kα line change with luminosity. In particular, for luminosities of 10^{45-46} erg s^{-1}, ionized iron lines have been detected in a few radio-quiet quasars (RQQs) (Nandra et al. 1996; Yamashita et al. 1997; George et al. 2000). At higher luminosities there is no evidence for any emission line at all (Nandra 1999; Vignali et al. 1999). Unfortunately, high-luminosity quasars are usually found at relatively high-redshift and therefore are rather weak in X–rays, making the study of spectral features extremely difficult.

High luminosity quasars differs from Seyfert 1s also in the observed shape of the X–ray continuum. Recent studies have suggested that high-redshift RQQs (Vignali et al. 1999) have flatter X–ray spectral slopes than lower redshift objects (George et al. 2000). However, it is not clear whether the spectral flattening is a function of redshift, implying a flattening of the continuum towards high energies, or rather it depends on the luminosity, thus suggesting a different emission mechanism at high luminosities.

Luminous radio-quiet quasars in the local Universe are rare. In this regard, PDS 456 is an exception and could provide hints on the nature of some of the properties described above, which are of great relevance to the physics of AGNs. PDS 456 is a bright (B=14.7) nearby (z = 0.184, Torres et al. 1997) radio-quiet quasar ($S_{1.4\ GHz}$ = 22.7 mJy, Condon et al. 1998; radio-loudness $R_L = -0.7$, Reeves et al. 2000) close to the Galactic plane (l = 10°.39, b=11°.16; $N_H \simeq 2 \times 10^{21}$ cm^{-2}, Dickey & Lockman 1990). The bolometric luminosity ($L \sim 10^{47}$ erg s^{-1}; Reeves et al. 2000) makes PDS 456 more luminous than the nearby (z = 0.158) radio-loud quasar 3C 273, without being jet-dominated. The ASCA and RXTE quasi-simultaneous observations discussed by Reeves et al. (2000) reveal the presence of a deep edge–like feature at E $>$ 8 keV which is likely to be due to highly ionized iron atoms. The 2–10 keV flux doubled

Send offprint requests to: C. Vignali

its intensity during a strong outburst which lasted for about 4 hours.

In order to further investigate the peculiar properties of this quasar we have carried out a medium–deep observation of PDS 456 with BeppoSAX. The results of the analysis are presented in Sect. 2, compared with a re-analysis of the ASCA observation in Sect. 3 and discussed in Sect. 4. Throughout the paper a Friedmann cosmology with $H_0 = 50\,\mathrm{km\,s^{-1}\ Mpc^{-1}}$ and $q_0 = 0.0$ is assumed.

2. BeppoSAX observation

2.1. Data reduction

The Italian-Dutch satellite BeppoSAX (Boella et al. 1997a) carries four co-aligned Narrow-Field Instruments (hereafter NFI), two of which are gas scintillation proportional counters with imaging capabilities: the Low Energy Concentrator Spectrometer (LECS, 0.1–10 keV, Parmar et al. 1997) and the Medium Energy Concentrator Spectrometer (MECS, 1.5–10 keV, Boella et al. 1997b). The remaining two instruments are the High Pressure Gas Scintillation Proportional Counter (HPGSPC, 4–120 keV, Manzo et al. 1997) and the Phoswich Detector System (PDS, 13–200 keV, Frontera et al. 1997). The quasar was observed by BeppoSAX on 1998 August 19–20. Data presented in this paper were obtained only with the imaging spectrometers, as PDS 456 has not been detected in the other two instruments. Standard reduction techniques and screening criteria were applied in order to produce useful linearized and equalized event files. A total of 62.7 ks and 29.7 ks have been accumulated for MECS and LECS instruments, respectively. Spectra have been extracted from circular regions of radius $4'$ and $6'$ around the source centroid for the MECS and LECS, respectively. Background spectra have been extracted from both blank-sky event files and from source-free regions in the target field-of-view. No apparent difference between the two spectra have been revealed. The background contributes to about 10% and 25% to the MECS and LECS count rates, the total net counts being $6.35\pm0.10 \times 10^{-2}$ in the 1.5–10 keV band and $2.12\pm0.09 \times 10^{-2}$ in the 0.4–4 keV energy range, respectively.

The XSPEC (version 10, Arnaud 1996) program has been extensively used to perform spectral analysis. In this paper errors are quoted at 90% confidence level for one interesting parameter ($\Delta\chi^2 = 2.71$, Avni 1976), and energies are reported in the source rest frame. In all our models, for both neutral and ionized absorbers, we assume solar abundances as tabulated in Anders & Grevesse (1989).

2.2. BeppoSAX spectral results

PDS 456 lies fairly close to the Galactic plane ($b \sim 11^\circ$). The Galactic H I column density derived by radio measurements is about $2\text{–}2.4 \times 10^{21}\,\mathrm{cm^{-2}}$ (Dickey & Lockman 1990; Stark et al. 1992). We have checked whether molecular hydrogen, traced by CO emission, is present towards the PDS 456 direction, with negative result (Lebrun & Huang 1984; Dame et al. 1987). Therefore a value of $3 \times 10^{21}\,\mathrm{cm^{-2}}$ (which is similar to the value found from the near-infrared observation of PDS 456 by Simpson et al. 1999) for the Galactic column density has been employed in all the spectral fits.

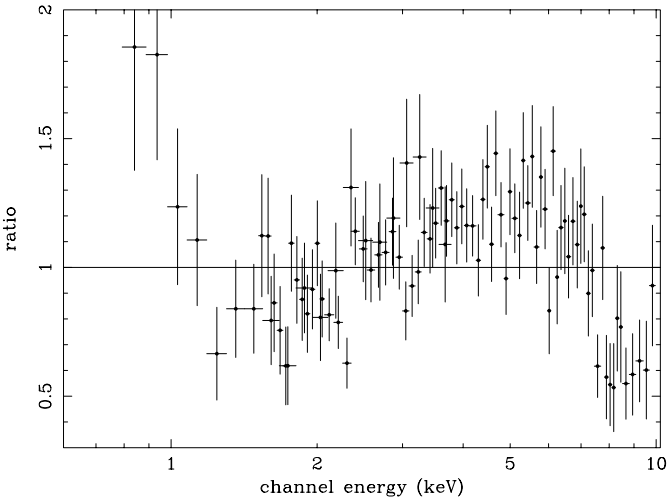

Fig. 1. The data/model residuals for a single power law fit to the LECS and MECS data.

The combined BeppoSAX MECS and LECS spectra were first fitted with a single power law plus Galactic absorption. The complexity of the spectrum is evident from the quality of the fit (χ^2/dof = 253/105) and from the data-to-model ratio (Fig. 1). This shows systematic deviations over the entire LECS+MECS band. In particular, an excess of counts below ~ 1 keV, as well as a strong deficit above 7–8 keV are clearly present, suggesting the presence of additional components at those energies. Furthermore, the monotonic rising of the model/counts ratio between ~ 1.5 and ~ 5 keV suggests that additional absorption, exceeding the Galactic value, is required.

To cure the strong residuals at energies above 7 keV (see Fig. 1) we added an absorption edge to the power law model (model **A** in Table 1). The improvement in the fit is highly significant ($\Delta\chi^2$/ Δdof = 110/2). The best-fit energy of the edge is consistent at 90% with that of the photoelectric K-edge of Fe XXIV–Fe XXVI. If this identification is correct, then the measured optical depth (see Table 1) implies that a high column density ($> 10^{24}\,\mathrm{cm^{-2}}$) of highly ionized matter is reprocessing the primary X–ray continuum of PDS 456 along our line of sight.

Though the fit is largely improved by the addition of the absorption edge, the χ^2 is still unacceptably high (143/103) and the residuals continue to show deviations at $E < 1$ keV. Moreover, the spectral index is very flat ($\Gamma = 0.94\pm0.07$). An acceptable fit and a more reasonable value for the power law slope ($\Gamma \simeq 1.3$) is obtained adding to model A two additional spectral components (model **B**): (a) an intrinsic neutral absorber obscuring the hard nuclear power law continuum, and (b) a soft power law, absorbed by the Galactic column density only. The best-fitting soft power law is very steep (though only poorly constrained: Table 1), indicating the presence of a luminous source of soft photons ($L_{0.5-2\ \mathrm{keV}} \simeq 5.2 \times 10^{44}\,\mathrm{erg\,s^{-1}}$) in the

Table 1. Results of BeppoSAX LECS (0.4–4 keV) and MECS (1.5–10 keV) spectral fits

Model	$\Gamma_{\rm soft}$	$N_{\rm H\ cold}$ (10^{22} cm^{-2})	$N_{\rm H\ warm}$ (10^{24} cm^{-2})	$\Gamma_{\rm hard}$	$\xi^{\rm a}$/LogU$^{\rm b}$	$E_{\rm edge}$ (keV)	τ	χ^2/dof
A	...	...	...	0.94 ± 0.07	...	8.77 ± 0.16	$1.23^{+0.26}_{-0.23}$	143/103
B	$3.95^{+0.78}_{-0.82}$	$2.40^{+1.40}_{-0.98}$	...	$1.29^{+0.18}_{-0.17}$	...	$8.82^{+0.21}_{-0.19}$	$0.98^{+0.28}_{-0.26}$	97/100
C	$3.99^{+0.76}_{-0.80}$	$2.77^{+1.29}_{-0.90}$	...	$1.61^{+0.20}_{-0.16}$	4230^{+14950}_{-2820}	...	...	94.2/100
D	3.95 ± 0.79	$2.67^{+1.34}_{-1.10}$	$4.47^{+2.77}_{-3.02}$	1.44 ± 0.17	$3.90^{+0.62}_{-0.56}$	...	...	94.7/100

[a] In units of erg cm s^{-1}

[b] U = $n_{\rm phot}/n_{\rm e}$ is the ionization parameter, defined as the ratio of the ionizing photons density at the surface of the cloud ($n_{\rm phot}$ = Q/(4πR^{2}c)) and the electron density of the gas.

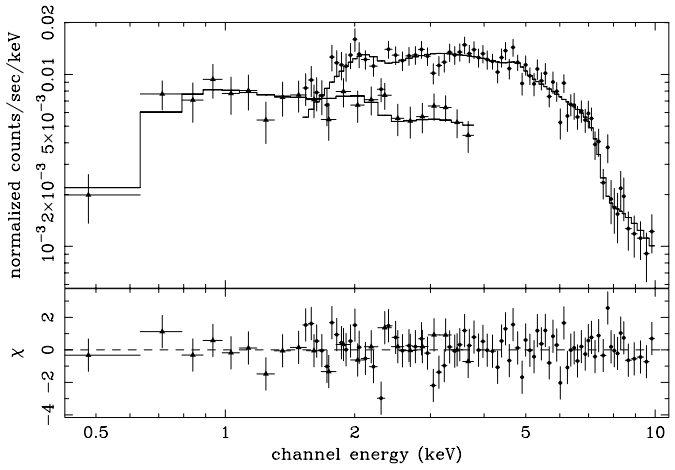

Fig. 2. The BeppoSAX spectrum (MECS+LECS, model **B**) and residuals

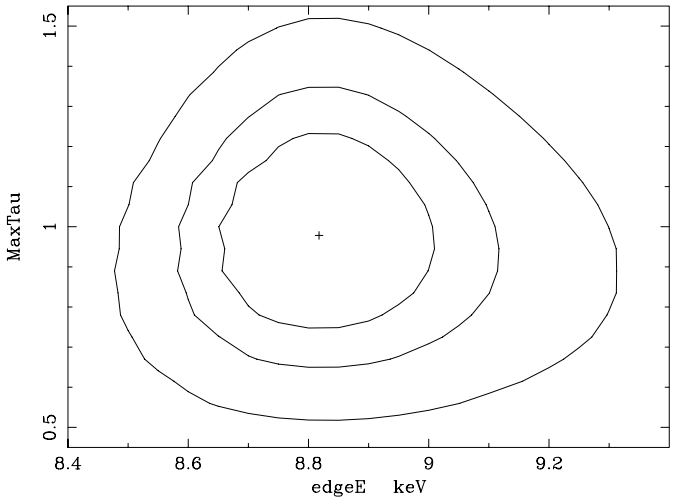

Fig. 3. 68, 90 and 99% edge energy – optical depth confidence contours (model **B**)

nuclear environment of PDS 456. The column density of neutral gas absorbing the hard X–ray power law largely exceedes the Galactic value along the line of sight to PDS 456, suggesting a "type-2-like" orientation for this high luminosity radio-quiet quasar.

The phenomenological model B provides a good fit to the observed 0.4–10 keV spectrum (Fig. 2) and good constraints to the various spectral parameters (Table 1, Fig. 3 and Fig. 4). To test the uniqueness of this model and to investigate whether the observed soft excess of photons, compared to the absorbed nuclear power law, is indeed due to genuine emission and not instead to an artifact due to additional complexity in the geometrical or physical status of the matter covering our line of sight to PDS 456, a few different spectral models were tested. More specifically, the soft X–ray power law was eliminated and the full-covering neutral absorber was either replaced by a partial covering absorber, allowing a fraction of the nuclear radiation to escape unabsorbed, or by a mildly ionized absorber transparent at energies lower than ~ 0.7 keV. None of these models was able to provide good quality fits to our data. We also replaced the soft power law with thermal emission from a collisionally ionized plasma, and refitted the data. This did not modify the best-fit parameters of the remaining spectral components, nor improved further the quality of the fit, compared to model B.

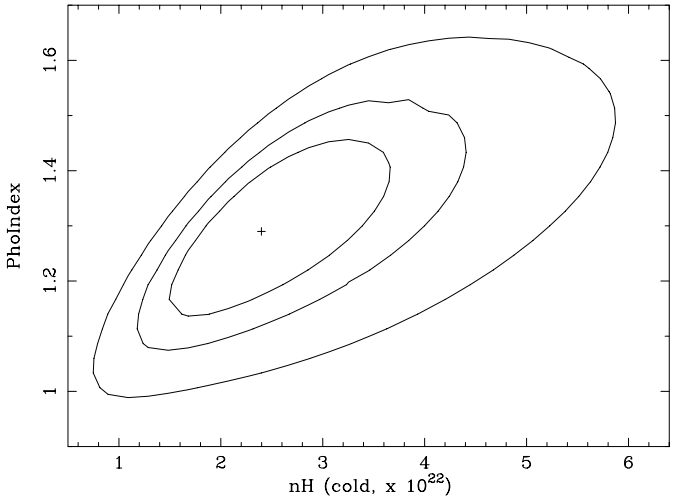

Fig. 4. Intrinsic cold $N_{\rm H}$ – Γ confidence contours for the model **B** in Table 1. Absorption in excess to the Galactic value is clearly present

Moreover, a significant contribution to the soft X–rays from starburst emission is unlikely. Indeed, given a 60–100 μm luminosity of 6–10 $\times$ 10^{45} erg cm^{-2} s^{-1} (depending on the assumed IR spectral slope) and relation [2] in David et al. (1992), only

about 5% of the soft X–ray emission may be due to star-forming emission. We then conclude that PDS 456 shows genuine soft X–ray emission below ~ 1 keV. Such a component is likely to be related to the strong UV bump present in the multiwavelength energy distribution (Reeves et al. 2000).

The energy and optical depth of the absorption edge in model B strongly suggest the presence of highly ionized gas absorbing and/or reflecting the primary radiation. To verify this hypothesys we then replaced the photoelectric edge in model B, with either an ionized reflector (parameterized by the model PEXRIV in XSPEC, Magdziarz & Zdziarski 1995: model **C**) or an ionized absorber (using the CLOUDY - Ferland 1996 - based model described in Nicastro et al. 2000a, and adopting the Mathews & Ferland 1987 parameterization for the AGN continuum: model **D**), and refitted the data. In both cases we left the soft and the hard, reflected/absorbed, power law free to vary independently. Both parameterizations gave acceptable χ^2. The best-fit values of $\Gamma_{\rm soft}$ and $\Gamma_{\rm hard}$ were consistent with each other between the two parameterizations. The hard reflected/absorbed continuum ($\Gamma \sim 1.4$–1.6) is still much flatter than the soft X–ray power law. Finally, the best-fit ionization parameters are consistent with each others, and their values correspond to a very high ionization state of the matter reflecting/absorbing the nuclear radiation, with iron mainly distributed among species XXI and XXVII. Both models provide then an acceptable description of our data. However, according to Matt et al. (1993), such a high ionized reflector should produce strong (EW $\sim$ 300–500 eV) fluorescence iron Kα emission lines at 6.7–6.97 keV. These lines are not observed in our data, the 90% upper limits on their equivalent width being of 120, 115 and 80 eV for neutral, He–like and H–like ionic species respectively. The corresponding 3σ limits lie in the range 150–180 eV. We then conclude that, while statistically acceptable, the model including an ionized reflector is not fully consistent with the BeppoSAX data of PDS 456. Kα emission from highly ionized iron is instead not expected to be strong in the case of an ionized absorber. The predicted strength of these lines depends on the fraction of solid angle covered by the absorber (as seen by the central source), and on the dynamics of the gas (see Sect. 4), but does not exceed few tens of eV for the strongest line, fully compatible with our data. A spectrum transmitted by a high column ($N_{\rm H_{warm}} \simeq 4.5 \times 10^{24}$ cm^{-2}) of highly ionized matter would then self-consistently account for both the observed deep absorption FeXXIV-XXVI K edge and the absence of Kα line emission from the same iron species (model D, Table 1).

The best-fit spectrum gives a 2–10 keV flux of about 5.7 $\times$ 10^{-12} erg s^{-1} cm^{-2}, which corresponds to an intrinsic 2–10 keV luminosity of about 1.2×10^{45} erg s^{-1}. At this flux level and given the relatively short exposure time, the source has not been detected at high energies by the PDS instrument (which spends about half of the time to monitor the background). In fact, a 3σ detection would have been possible only for a power law harder that $\Gamma \simeq 1.3$ (Guainazzi & Matteuzzi 1997). The present upper limit provides therefore only a loose contraint on the high energy spectrum.

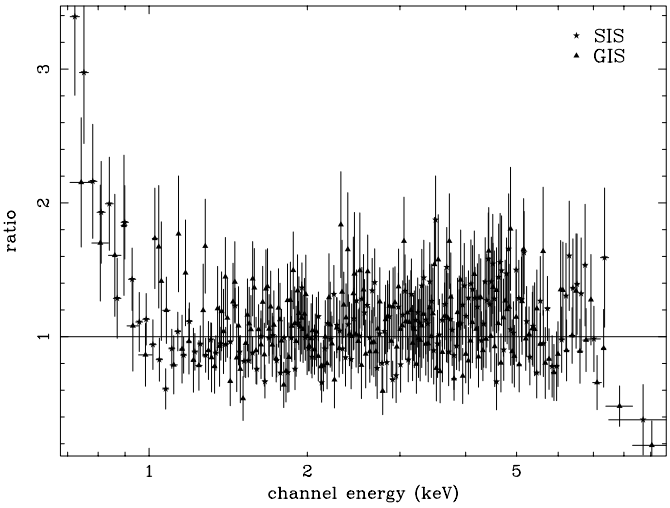

Fig. 5. The residuals obtained by fitting the ASCA spectrum with a single power law. The soft excess at E $<$ 1 keV and the counts deficit at E $>$ 7 keV are similar to the BeppoSAX data.

3. ASCA observation

3.1. Data reduction

PDS 456 was observed by the ASCA satellite (Tanaka et al. 1994) on 1998 March 7 during the AO6 phase. The focal plane instruments consist of two solid-state imaging spectrometers (SIS, Gendreau 1995) and two gas scintillation imaging spectrometers (GIS, Makishima et al. 1996), characterized by a good spectral resolution (about 2% and $\sim$ 8% at 5.9 keV, respectively) and broad-band ($\sim$ 0.6–10 keV) capabilities. The observations were performed in FAINT mode and then corrected for dark frame error and echo uncertainties as suggested by Otani & Dotani (1994). The data were screened with the version 1.4b of the XSELECT package with standard criteria. The final observing time is about 41 ks for both SIS and GIS detectors. Source counts were extracted from circles of 6′ radius for GIS and 3′.5 for SIS centered on the source, and background spectra were extracted from source-free regions from the same CCD chip for SIS and from the same field of view for GIS. The source count rates (after background-subtraction) are 6.90$\pm$0.11 $\times$ 10^{-2} and 6.13$\pm$0.11 $\times$ 10^{-2} counts per second for SIS and GIS, respectively.

3.2. ASCA spectral results

SIS and GIS data were fitted simultaneously allowing the relative normalizations to be free to vary, to account for residual discrepancies in the absolute flux calibration. The residuals of a single power law fit ($\Gamma = 1.48 \pm 0.04$, Fig. 5) are similar to those of BeppoSAX and fully consistent with the results reported by Reeves & Turner (2000) in their analysis of the same ASCA data. In particular, a soft excess and an edge appear prominently. No emission line has been detected. The 90% upper limits for the neutral, He–like and H–like lines are in the 45–70 eV range while, the 3σ upper limits are of the order of 100–130 eV.

The presence of an ionized edge is fully confirmed by ASCA data ($\Delta\chi^2/\Delta$dof = 47/2 with respect to a single power law model). The edge spectral parameters are consistent with the BeppoSAX observation but less constrained due to the lower ASCA effective area at E $>$ 7 keV. At low-energies, the spectrum clearly shows a soft component. The addition of a power law improves the fit.

Looking for consistency between the BeppoSAX and the ASCA data of PDS 456, we then fitted our chosen parameterization of the BeppoSAX data (model D) to the ASCA data. The edge is fully accounted for by this model. Both the ionization parameter and the warm absorbing column density are in agreement with BeppoSAX values. The ASCA data require a steeper spectral slope ($\Gamma_{\mathbf{H}} \simeq 1.6$–$2.0$) and a moderately lower neutral column density, but consistent, within the errors, with the BeppoSAX results.

4. Discussion

ASCA and BeppoSAX observations of PDS 456 were taken about 5 months (observer frame) apart. The flux level of the source was lower during the ASCA observation ($F_{2-10\ \mathrm{keV}} \simeq 3.6 \times 10^{-12}$ erg cm^{-2} s^{-1}) than during the BeppoSAX one ($F_{2-10\ \mathrm{keV}} \simeq 5.7 \times 10^{-12}$ erg cm^{-2} s^{-1}). A 50% flux variation over 3 days has been detected by RXTE during a quasi–simultaneous observation with ASCA. The RXTE range of fluxes encompass the ASCA and BeppoSAX measurements. In addition, a strong flare with a doubling time of about 17 ksec is present in the RXTE observation (Reeves et al. 2000). The underlying continuum of the ASCA/RXTE spectrum ($\Gamma \simeq 2.3$–2.4) is steeper than the slope obtained from the present analysis of BeppoSAX and ASCA data and from the independent analysis of the ASCA spectrum discussed in Reeves & Turner (2000). The origin of such a discrepancy is unclear. Intercalibration errors between RXTE and ASCA and/or a significant steepening of the continuum spectrum above 10 keV may provide a plausible explanation.

The presence of a prominent ionized iron K edge, with similar values for the best-fit energy and optical depth in RXTE and BeppoSAX data, represents the most striking observed feature in PDS 456 and unambiguously points to a highly ionized nuclear environment in this quasar. The edge parameters are equally well reproduced by either reflection off or transmission through a highly ionized gas. In the first case the ionization status inferred from the edge energy would imply a strong ($\sim$ 300–500 eV; Matt et al. 1993) ionized (6.7–6.97 keV) iron line. If the edge originates in a high column density (N_{H} a few 10^{24} cm^{-2}) warm gas, no strong iron line is expected (see below). The BeppoSAX and ASCA upper limits on the line intensity derived from the present analysis would then favour a transmission model. On the other hand, the tentative detection of a broad iron line in the RXTE data ($\sigma \sim 1$ keV, EW $\sim$ 350 eV) would instead favour the reflection scenario (Reeves et al. 2000).

To further investigate the properties of the high column density, highly ionized absorber we have carried out more detailed calculations using the photoionization models described in Nicastro et al. (1999) and Nicastro et al. (2000a), which includes photoelectric and resonant absorption as well as gas emission. The best-fit value of the ionization parameter implies that the iron atoms are equally distributed among the 3 highest ionization states: Fe XXV ($\sim$ 30%), Fe XXVI ($\sim$ 40%) and Fe XXVII (i.e. fully ionized, $\sim$ 30%). In a spherical configuration, the net intensity of the corresponding emission lines depends (a) on the fraction of solid angle (as seen by the central source) covered by the absorber/emitter, and (b) the ratio between the outflowing (v_{out}) and the turbolence (v_{turb}) gas velocities. We then ran our models for different values of the covering factor between 0.1 and 1. To maximize the net contribute of line emission, compared to absorption, we used $v_{\mathrm{out}}/v_{\mathrm{turb}} = 5$, which guarantees a peak-to-peak separation of absorption and emission lines by the same transition greater than 3 times the width of these features (Nicastro et al. 2000b). The rather uncertain knowledge of the dynamical status of the gas prevents us from a more detailed treatment. The results indicate that the total equivalent width of the line blend (including recombination, fluorescent and intercombination lines) never exceeds $\sim$100 eV, a value lower than the upper limits derived from ASCA and BeppoSAX data, leading further support to the transmission model. Finally, the 0.1–2 keV continuum-plus-line fluxes predicted by these models allowed us to estimate the maximum contribution of gas emission to the soft component measured in both the BeppoSAX and ASCA data to be not larger than $\sim$ 20%.

5. Conclusions

The most important results obtained from the BeppoSAX observation of the luminous quasar PDS 456 can be summarized as follows:

- The BeppoSAX observation confirms the presence of a deep ionized K edge discovered by RXTE at $\sim$ 8.5–9 keV implying the presence of highly ionized gas around the central source.
- The absence of significant iron line emission in both the BeppoSAX and ASCA data favours a model where the hard X–ray continuum is absorbed by a high column density of highly ionized gas. Further spectral complexity is present at lower energies, requiring the presence of an additional cold (or weakly ionized) absorber.
- The high luminosity of PDS 456 ($L_{\mathrm{bol}} \sim 10^{47}$ erg s^{-1}) and the properties of the absorbing medium which partially hides the X–ray source make this object a good candidate to test the emission mechanisms and reprocessing in quasars.

Further investigations with CHANDRA and XMM would be extremely helpful to assess the nature of the X–ray emission (both in the soft and in hard X–rays domain) and the ionization state of the absorbing matter. Moreover, X–ray spectroscopy of others bright, relatively nearby quasars would be very important to check whether PDS 456 is an exceptional object or the imprints of highly ionized high column density gas are common in luminous quasars. A better knowledge of the X–ray properties of bright AGN would also allow to probe the physics of accretion processes at high luminosities.

Acknowledgements. We thank all the people who, at all levels, have made possible the BeppoSAX mission. We also thank all the members of the ASCA team who operate the satellite and maintain the software and database. This work has made use of the NASA/IPAC Extragalactic Database (NED) which is operated by the Jet Propulsion Laboratory, Caltech, under contract with the National Aereonautics and Space Administration, of data obtained through the High Energy Astrophysics Science Archive Research Center Online Service, provided by the Goddard Space Flight Center and of the Simbad database, operated at CDS, Strasbourg, France. The authors would like to thank the referee, S. Komossa, for her suggestions who improved the quality of the paper. Financial support from Italian Space Agency under the contract ARS–98–119 is ackowledged by C. V., A. C and G.G.C. P. This work was partly supported by the Italian Ministry for University and Research (MURST) under grant Cofin98-02-32. F.N. Aknowledges the NASA grant NAG5-9216.

References

Anders E., Grevesse N., 1989, Geochimica et Cosmochimica Acta 53, 197
Arnaud K.A., 1996, In: Jacoby G., Barnes J. (eds.) Astronomical Data Analysis Software and Systems V, ASP Conf. Series vol. 101, p. 17
Avni Y., 1976, ApJ 210, 642
Boella G., Butler R.C., Perola G.C., et al., 1997a, A&AS 122, 299
Boella G., Chiappetti L., Conti G., et al., 1997b, A&AS 122, 327
Comastri A., Setti G., Zamorani G., et al., 1992, ApJ 384, 62
Condon J.J., Cotton W.D., Greisen E.W., et al., 1998, AJ 115, 1693
Dame T.M., Ungerechts H., Cohen R.S., et al., 1987, ApJ 322, 706
David L.P., Jones C., Forman W., 1992, ApJ 388, 825
Dickey J.M., Lockman F.J., 1990, ARA&A 28, 215
Ferland G.J., 1996, CLOUDY: 90.01
Frontera F., Costa E., Piro L., et al., 1997, A&AS 122, 357
Gendreau K., 1995, Ph.D. Thesis, Massachussetts Institute of Technology
George I.M., Turner T.J., Yaqoob T., et al., 2000, ApJ 531, 52
Guainazzi M., Matteuzzi A., 1997, SDC Technical Report
Iwasawa K., Taniguchi Y., 1993, ApJ 413, L15
Lawson A.J., Turner M.J.L., Williams O.R., et al., 1992, MNRAS 259, 743
Lawson A.J., Turner M.J.L., 1997, MNRAS 288, 920
Lebrun F., Huang Y.-L., 1984, ApJ 281, 634
Magdziarz P., Zdziarski A.A., 1995, MNRAS 273, 837
Makishima K., Tashiro M., Ebisawa K., et al., 1996, PASJ 48, 171
Manzo G., Giarrusso S., Santangelo A., et al., 1997, A&AS 122, 341
Mathews W.G., Ferland G.J., 1987, ApJ 323, 456
Matt G., Fabian A.C., Ross R.R., 1993, MNRAS 262, 179
Nandra K., Pounds K.A., 1994, MNRAS 268, 405
Nandra K., George I.M., Turner T.J., Fukazawa Y., 1996, ApJ 464, 165
Nandra K., George I.M., Mushotzky R.F., Turner T.J., Yaqoob T., 1997, ApJ 476, 70
Nandra K., 1999, In: Ferland G., Baldwin J. (eds.) Quasars and Cosmology. ASP Conf. Series Vol. 162, p. 65
Nicastro F., Fiore F., Matt G., 1999, ApJ 517, 108
Nicastro F., Piro L., De Rosa A., et al., 2000a, ApJ 536, 718
Nicastro F., Elvis M., Fiore F., Matt G., Savaglio S., 2000b, Proceedings of the Conference X–ray Astronomy '99: Stellar Endpoints, AGNs and the Diffuse X–ray Background
Otani C., Dotani T., 1994, ASCA Newsl. 2, 25
Parmar A.N., Martin D.D.E., Bavdaz M., et al., 1997, A&AS 122, 309
Reeves J.N., Turner M.J.L., Ohashi T., Kii T., 1997, MNRAS 292, 468
Reeves J.N., O'Brien P., Vaughan S., et al., 2000, MNRAS 312, L17
Reeves J.N., Turner M.J.L., 2000, MNRAS 316, 234
Simpson C., Ward M., O'Brien P., Reeves J., 1999, MNRAS 303, L23
Stark A.A., Gammie C.F., Wilson R.W., et al., 1992, ApJS 79, 77
Tanaka Y., Inoue H., Holt S.S., 1994, PASJ 46, L37
Torres C.A.O., Quast G.R., Coziol R., et al., 1997, ApJ 488, L19
Vignali C., Comastri A., Cappi M., et al., 1999, ApJ 516, 590
Williams O.R., Turner M.J.L., Stewart G.C., et al., 1992, ApJ 389, 157
Yamashita A., Matsumoto C., Ishida M., et al., 1997, ApJ 486, 763